Electronic Supplementary Material (ESI) for RSC Advances.

Supporting Information

Effect of Carbon Nanosheets with Different Graphitization Degree as Support of Noble Metal on Selective Hydrogenation of Cinnamaldehyde

Qing Han, Yunfei Liu, Dong Wang, Fulong Yuan, Xiaoyu Niu*, Yujun Zhu*

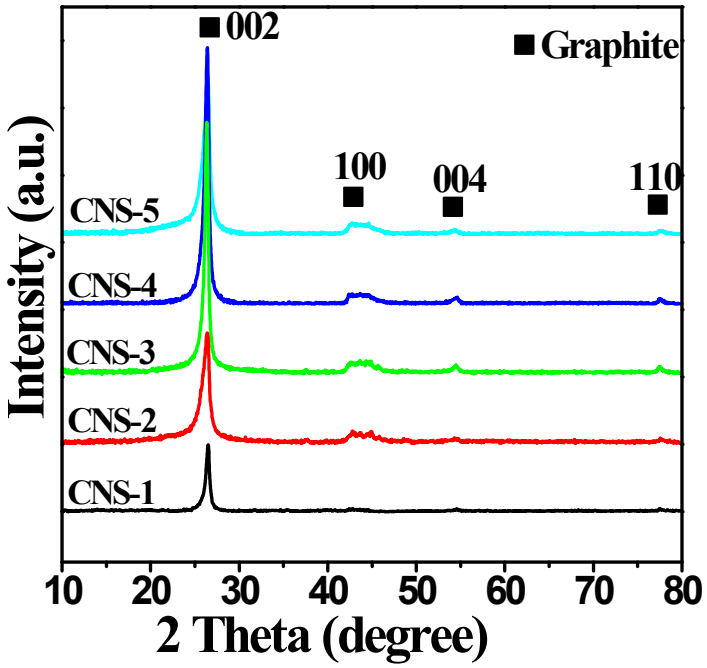

Fig. S1 XRD patterns of CNS-1, CNS-2, CNS-3, CNS-4 and CNS-5 supports

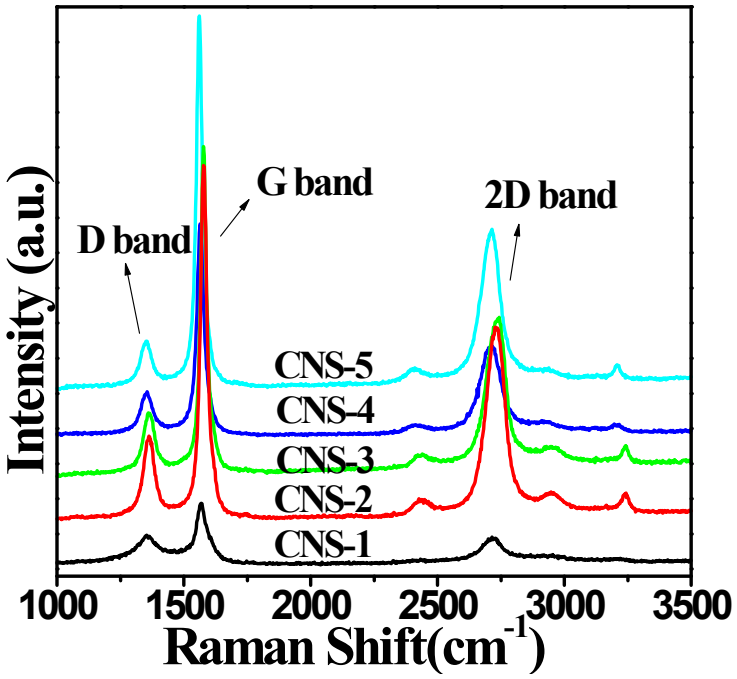

Fig. S2 Raman spectra of CNS-1, CNS-2, CNS-3, CNS-4 and CNS-5 supports

SEM can be intuitived to observe the morphology of the sample. Fig. S3 showed SEM images of five Pt/CNS samples. Fig. S3b, d, f, h and j are the further enlarge images of Fig. S3a, c, e, g and i, respectively.

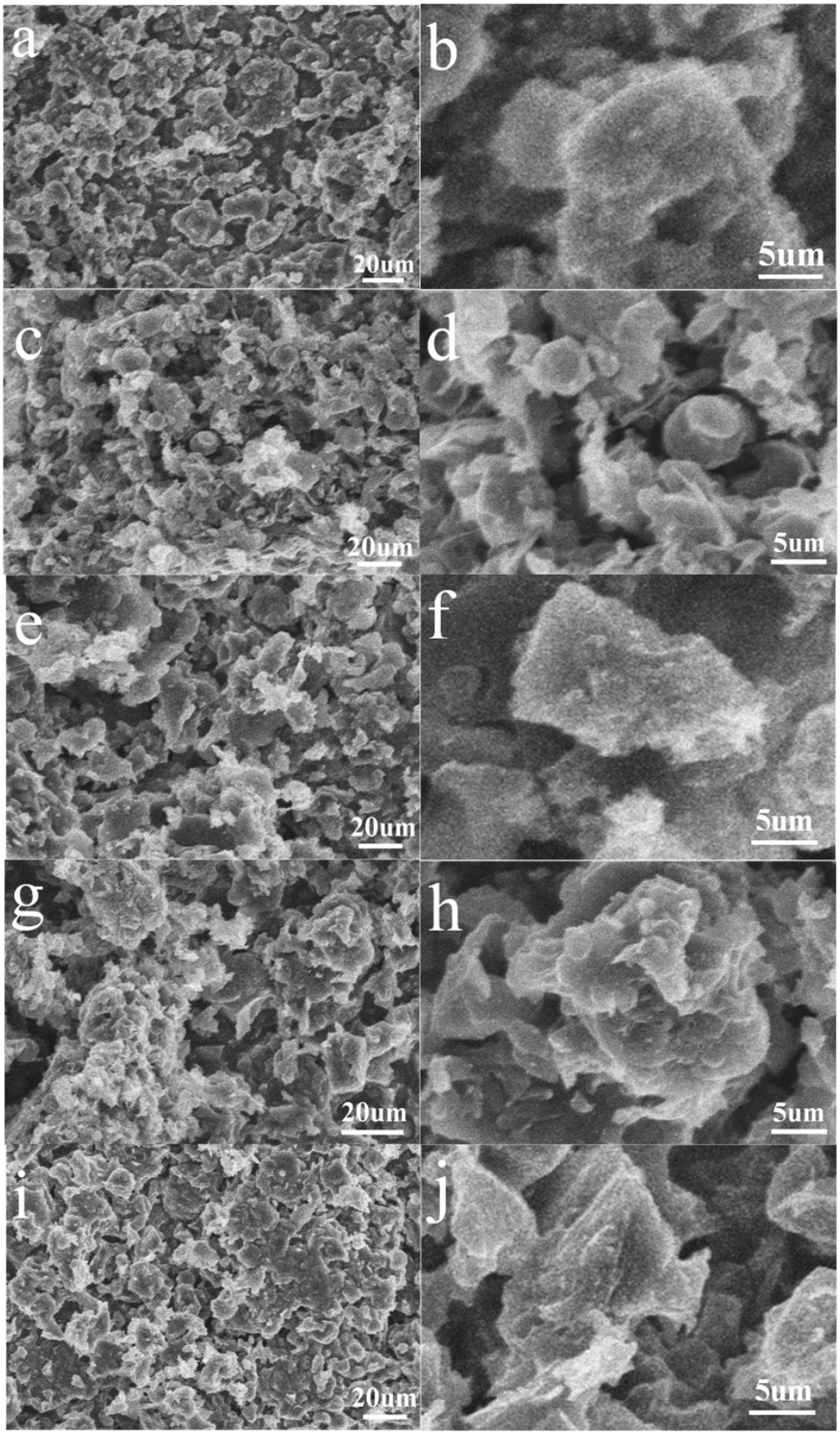

Fig. S3 SEM images of (a, b) CNS-1, (c, d) CNS-2, (e, f) CNS-3, (g, h) CNS-4, (i, j) CNS-5 supports.

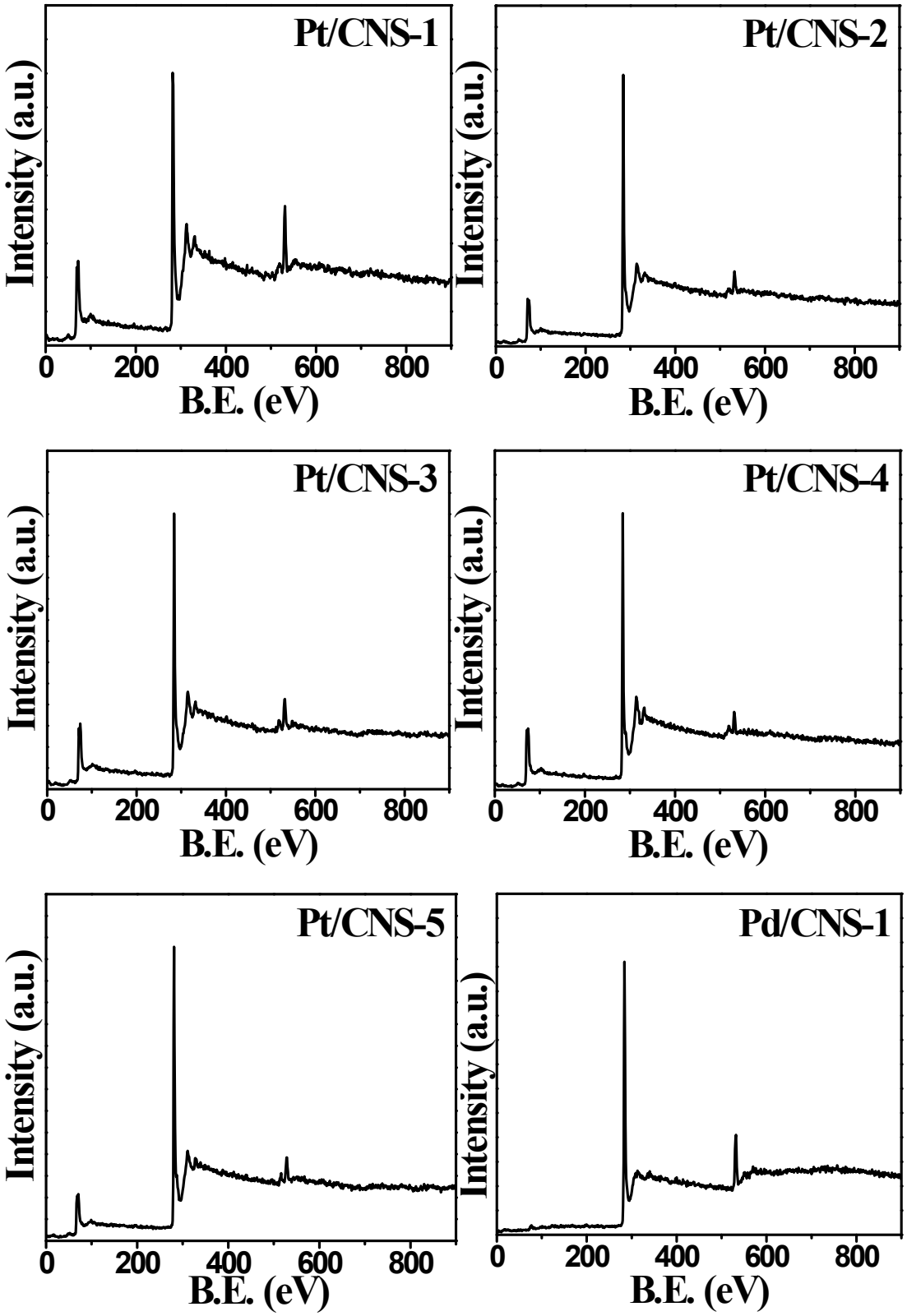
Pt/CNS-1
Intensity (a.u.)
0
200
400
600
800
B.E. (eV)
Pt/CNS-2
Intensity (a.u.)
0
200
400
600
800
B.E. (eV)
Pt/CNS-3
Intensity (a.u.)
0
200
400
600
800
B.E. (eV)
Pt/CNS-4
Intensity (a.u.)
0
200
400
600
800
B.E. (eV)
Pt/CNS-5
Intensity (a.u.)
0
200
400
600
800
B.E. (eV)
Pd/CNS-1
Intensity (a.u.)
0
200
400
600
800
B.E. (eV)

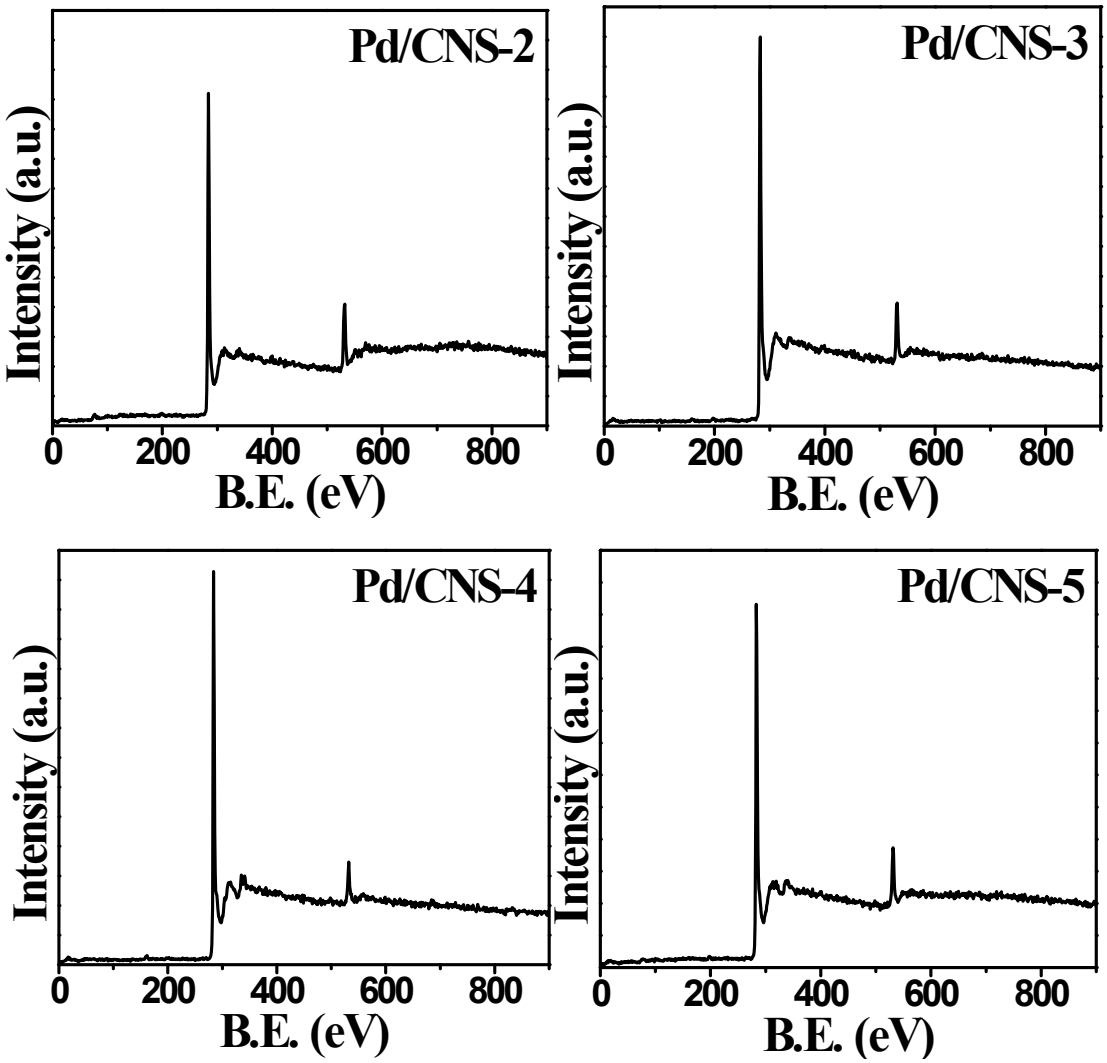

Fig. S4 XPS spectra of Pt/CNS and Pd/CNS catalysts.

Diffraction peaks observed in the patterns of all catalysts at 2θ = 39.7, 45.6, and 66.8 ° can be assigned to the crystalline planes (111), (200), and (220) of the face-centered cubic Pd nanoparticles, respectively **(**Fig. S5). The averaged crystal sizes of Pd nanoparticles calculated by full width at half maximum of Pd (111) reflection based on Scherrer's equation are 9.7, 10.2, 10.1, 10.0 and 9.8 nm for Pd/GNS-1, Pd/GNS-2, Pd/GNS-3, Pd/GNS-4, and Pd/GNS-5 samples, respectively. Similar mean particle size (~ 10 nm) of Pd was obtained for all Pd/CNS catalysts.

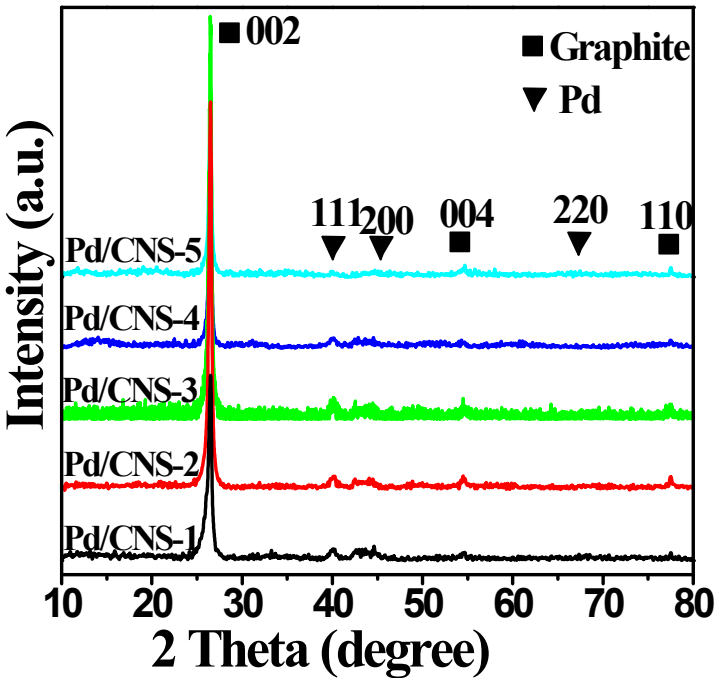

Fig. S5 XRD patterns of Pd/CNS-1, Pd/CNS-2, Pd/CNS-3, Pd/CNS-4 and Pd/CNS-5 catalysts.

The electronic structure of Pd in the Pd/CNS catalysts was also determined using XPS analysis (Fig. S6). It is clear that Pd 3d spectra of the Pd/CNS could be deconvolved into two spin-split states, as summarized in Table S1. The first doublet (335.4 and 340.8 eV) and the second doublet (337.7 and 342.9 eV) can be assigned to metallic Pd^0 and Pd^{2+} , respectively. The binding energy of metallic Pd^0 is high due to Pd-C strong interaction, resulting in a fast electron transfer from Pd to CNS. In terms of quantitation of the composition of the Pd nanoparticles, the content of the surface Pd^0 and Pd^{2+} species in Pd/CNS-5 catalysts was estimated to be 62.4 and 37.6% (Table S1).

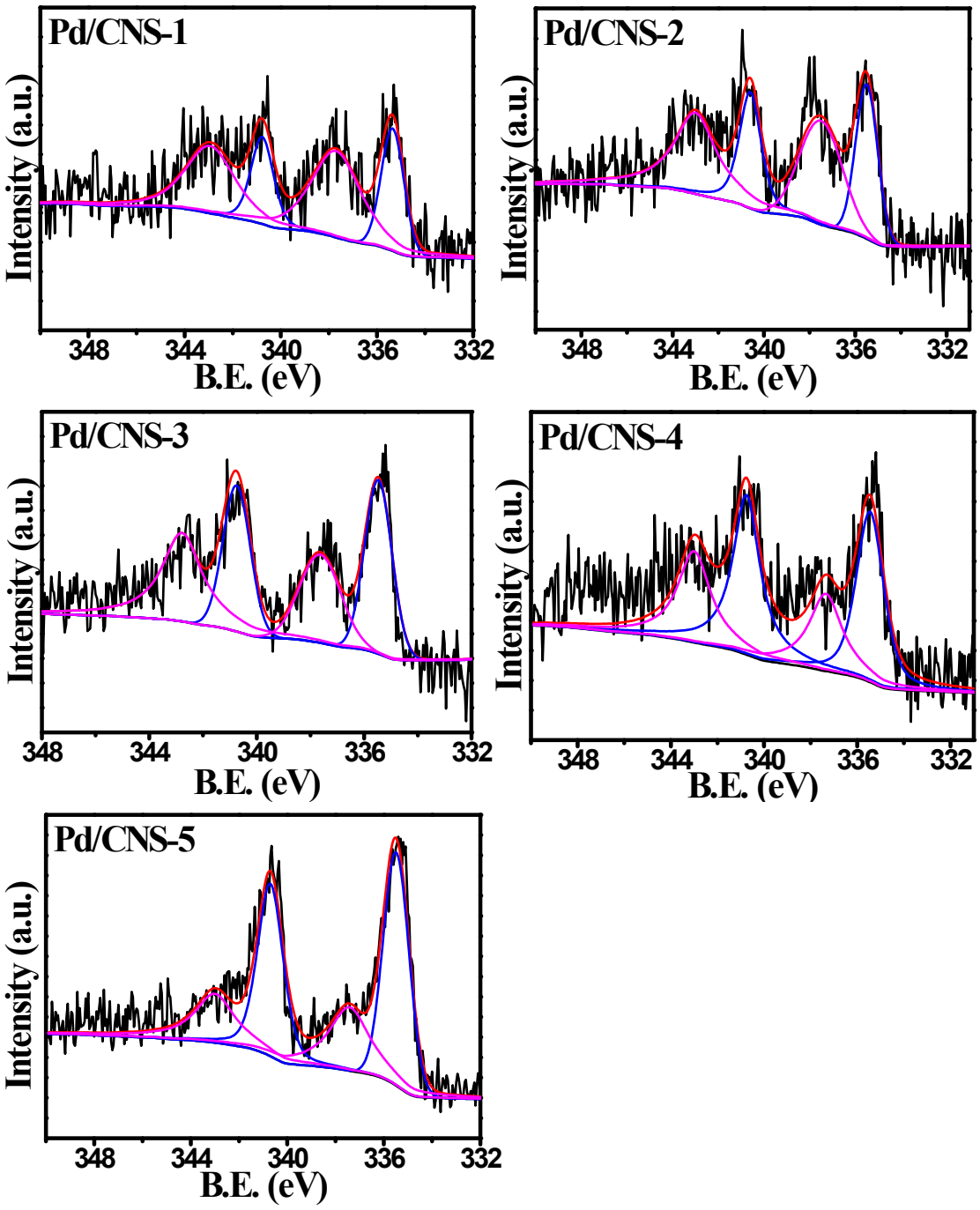

Fig. S6 The Pd 3d high-resolution XPS spectra of Pd/CNS-1, Pd/CNS-2, Pd/CNS-3, Pd/CNS-4, and Pd/CNS-5 catalysts.

Table S1 XPS date of the Pd 3d levels for the different catalysis.

Catalysis	Pd species	Pd species BE(eV)		Content of Pd species(%)
		$3d_{5/2}$	$3d_{3/2}$	
3.5 wt% Pd/CNS-1	Pd^0	335.4	340.8	32.5
	Pd^{2+}	337.7	342.9	67.5
3.5 wt% Pd/CNS-2	Pd^0	335.5	340.6	40.7
	Pd^{2+}	337.4	343.0	59.3
3.5 wt% Pd/CNS-3	Pd^0	335.5	343.8	49.4
	Pd^{2+}	337.7	342.8	50.6
3.5 wt% Pd/CNS-4	Pd^0	335.5	340.8	59.6
	Pd^{2+}	337.4	343.0	40.4
3.5 wt% Pd/CNS-5	Pd^0	335.5	340.7	62.4
	Pd^{2+}	337.4	343.0	37.6